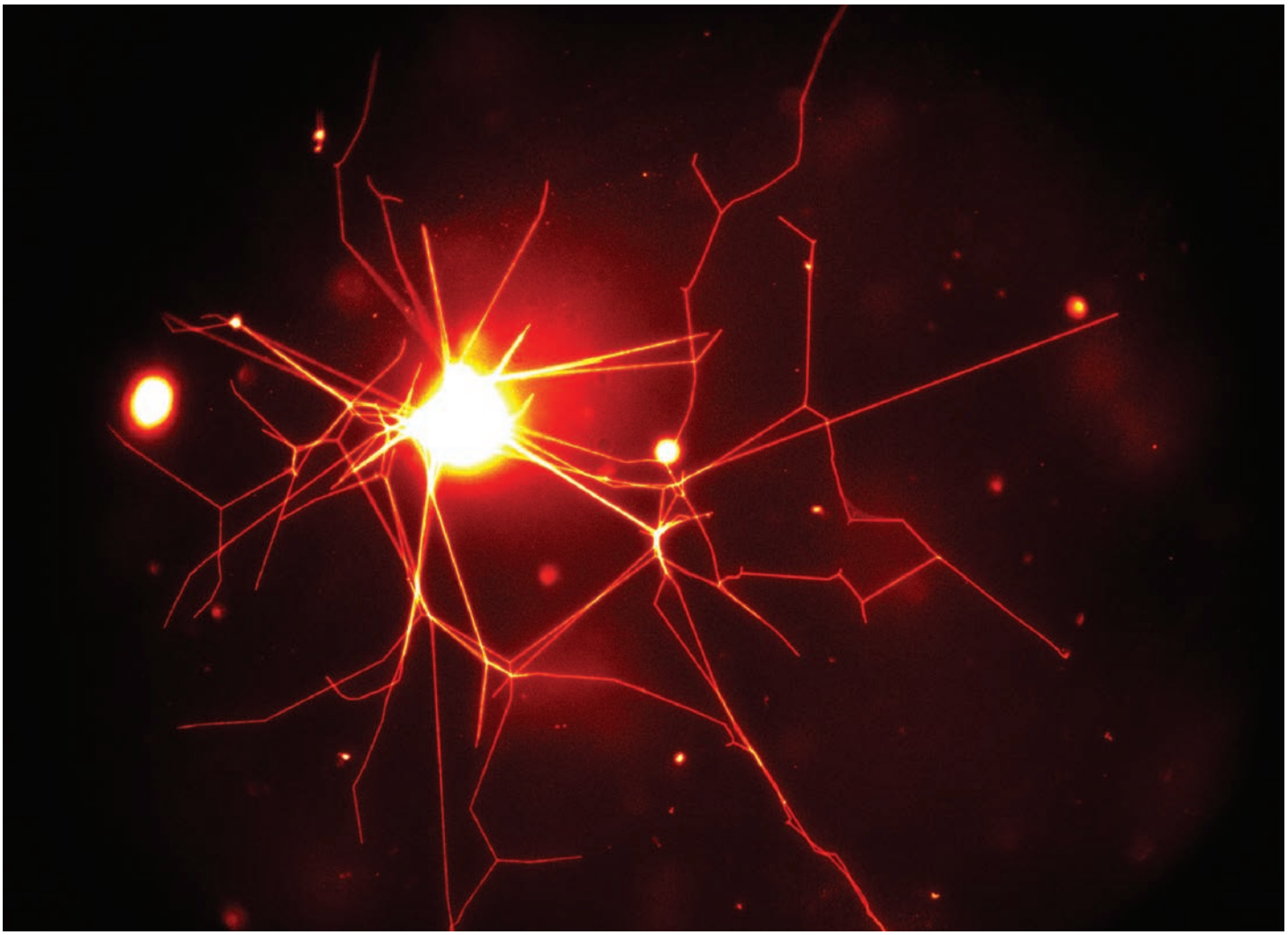

Showcasing research from the Center for Integrated Nanotechnologies, Sandia National Laboratories, Albuquerque, NM.

Dynamic assembly of polymer nanotube networks *via* kinesin powered microtubule filaments

Paxton, Bachand, and coworkers describe for the first time how biological nanomotors may be used to actively self-assemble mesoscale networks composed of diblock copolymer nanotubes. The collective force generated by multiple kinesin nanomotors acting on a microtubule filament is large enough to overcome the energy barrier required to extract nanotubes from polymer vesicles comprised of poly(ethylene oxide-*b*-butadiene) in spite of the higher force requirements relative to extracting nanotubes from lipid vesicles.

As featured in:

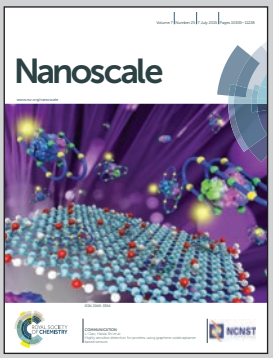

See Walter F. Paxton, George D. Bachand *et al.* *Nanoscale*, 2015, **7**, 10998.

ROYAL SOCIETY OF CHEMISTRY

www.rsc.org/nanoscale

Registered charity number: 207890

Nanoscale

PAPER

View Article Online
View Journal | View Issue

Published on 24 April 2015. Downloaded by Michigan State University on 20/01/2016 02:28:09.

Cite this: *Nanoscale*, 2015, **7**, 10998

Dynamic assembly of polymer nanotube networks *via* kinesin powered microtubule filaments†

Walter F. Paxton,* Nathan F. Bouxsein, Ian M. Henderson, Andrew Gomez and George D. Bachand*

Received 4th February 2015,
Accepted 20th April 2015

DOI: 10.1039/c5nr00826c

www.rsc.org/nanoscale

We describe for the first time how biological nanomotors may be used to actively self-assemble meso-scale networks composed of diblock copolymer nanotubes. The collective force generated by multiple kinesin nanomotors acting on a microtubule filament is large enough to overcome the energy barrier required to extract nanotubes from polymer vesicles comprised of poly(ethylene oxide-*b*-butadiene) in spite of the higher force requirements relative to extracting nanotubes from lipid vesicles. Nevertheless, large-scale polymer networks were dynamically assembled by the motors. These networks displayed enhanced robustness, persisting more than 24 h post-assembly (compared to 4–5 h for corresponding lipid networks). The transport of materials in and on the polymer membranes differs substantially from the transport on analogous lipid networks. Specifically, our data suggest that polymer mobility in nanotubular structures is considerably different from planar or 3D structures, and is stunted by 1D confinement of the polymer subunits. Moreover, quantum dots adsorbed onto polymer nanotubes are completely immobile, which is related to this 1D confinement effect and is in stark contrast to the highly fluid transport observed on lipid tubules.

Introduction

The ability to control the association of dynamic soft materials into intricate assemblies that mimic biological structures offers the potential for tremendous control over the micro- and nanoscale transport of materials. Tubular structures from organelles such as the smooth endoplasmic reticulum are common in eukaryotic cells and function as useful conduits for the transport of small molecules.[1] The assembly and spatial organization of these organelles is controlled by cytoskeletal motor proteins acting on lipid membranes, generating structures that are highly non-equilibrium. Similar microscale structures may be generated *ex vivo* using the natural motility of kinesin motors moving along microtubule filaments.[2–4] In contrast, we recently demonstrated the active assembly of millimeter-scale lipid nanotube networks using the kinesin-driven motion of microtubule filaments.[5] Whereas serial processes such as pipet micromanipulation[6] and optical tweezing[7] allow precision control over nanotube networks, the autonomous motion of individual microtubules by kinesin motors allows for the highly parallel formation of large networks on a relatively short timescale (*i.e.*, minutes). This approach thus enables considerable enhancement in the complexity of lipid networks while also greatly decreasing the time required to form them. Such tubular structures have the potential to enable rapid and efficient transfer of matter and information across multiple length-scales in a directed manner that circumvents the losses of normal three-dimensional diffusive processes.

The utility of tubular highways comprising these networks, however, may be limited by the inherent instability of the lipid assemblies. Applications that require networks to persist longer than a few hours or those that require convective flows would not be suitable for lipid-based networks based on their mechanical instability. For example, networks used as physical models to study the transport of matter[8] or communication[9] between cells may require both extended experiment times and the introduction of solutions by flow that cannot be achieved with lipid nanotubes. Furthermore, materials applications, such as the integration of networks at a biotic/abiotic interface, would have even more stringent requirements for stability.

Block copolymer amphiphiles on the other hand have been highly regarded as robust synthetic analogues of lipid-based materials, as they display similar physical behaviors but with increased stability.[10–12] Therefore, the goal of the current work was to develop polymer nanotubular networks using

Center for Integrated Nanotechnologies, Sandia National Laboratories, Albuquerque, NM 87185, USA. E-mail: wfpaxto@sandia.gov, gdbacha@sandia.gov

†Electronic supplementary information (ESI) available: Fluorescence video microscopy of the kinesin-powered microtubule extracting nanotubes from multilamellar vesicles to produce polymer nanotube networks from (1) $EO_{21}Bd_{32}$ or (2) $EO_{21}Bd_{32}$ with 0.5% added lipid. See DOI: 10.1039/c5nr00826c

This journal is © The Royal Society of Chemistry 2015

Published on 24 April 2015. Downloaded by Michigan State University on 20/01/2016 02:28:09.

biomolecular active transport. To this end, we investigated the ability of the kinesin/microtubule system to prepare bifurcated, networked structures from polymer-based amphiphiles comprising multilamellar polymer vesicles. We chose poly(ethylene oxide)-*b*-poly(butadiene) because it is one of the most widely studied vesicle-forming polymers, and many of the relevant physical properties of the resulting membranes they form are known. The resulting polymer networks persist considerably longer than lipid networks, owing to the comparative stability of the polymer membranes. The ability of these polymer systems to support the transport of materials along these soft, tubular structures was also evaluated. Our work demonstrates that the collective action of kinesin motors produces forces that are large enough to extract nanotubes from polymer vesicles, forming networks with similar size and morphology to those generated from lipid vesicles. This development substantially increases the library of soft amphiphilic materials that may be used to rapidly form large-scale nanotube networks. Furthermore, we demonstrate that the use of polymer amphiphiles in this system introduces anomalies in membrane-based transport that should be considered when designing soft, tubular highways for transport in biomimetic systems.

Results and discussion

Polymer nanotube networks were formed within 30 min using a kinesin/microtubule inverted motility assay (Fig. 1) from multilamellar vesicles comprised of an amphiphilic block copolymer – poly(ethylene oxide)$_{21}$-*b*-poly(butadiene)$_{32}$ ($EO_{21}Bd_{32}$) – with a fraction of the polymer chains end-functionalized with biotin (8%). Visualization was enabled by the addition of 0.5% fluorescent polymer (tetramethylrhodamine-labeled $EO_{21}Bd_{32}$; Fig. 1B) or lipid (Texas Red DHPE; Fig. 1C). Under the same conditions, polymer-only networks were generally smaller, less common, and less bifurcated than either lipid-only networks or polymer networks that included the lipid-dye TR-DHPE. The larger force requirements for creating polymer networks (discussed below) likely accounts for this apparent difference, which may be alleviated by a small amount of added lipid (0.5%), similar to the addition of a fluidizing agent to polymer vesicles reported previously.[13] Importantly, our motor-driven approach yields robust polymer networks, with or without added lipid, that persist in excess of 24 h, compared to lipid nanotube networks with lifetimes that rarely exceed 4–5 h. This stability of the polymer nanotube networks is consistent with the enhanced mechanical stability characteristic of polymer bilayer systems.[10,11]

Given the enhanced stability of polymer bilayers and their considerable physical differences relative to lipid bilayers, the ability to pull nanotubes from vesicles composed entirely of polymer using the inverted motility assay was somewhat surprising. The force required to pull nanotubes from vesicles includes the barrier force related to the initial deformation of the membrane and a dynamic pulling force due to extending the length of the extracted bilayer nanotube.[14] In our experiments, the barrier force is comparable to the pulling force.‡ As a result, the dynamic pulling is the dominant contributor to the required force, which is expected to scale with (i) the square of the membrane thickness and (ii) an interfacial coupling constant that accounts for the mechanical coupling between the inner and outer leaflets of a bilayer membrane.[15] The polymers used in our experiments have a bilayer thickness of ~8 nm[16,17] compared to ~2.7 nm for DOPC bilayers.[18] As a result, the required force due to differences in thickness is 8–9× greater for polymer bilayers. The interfacial coupling effect§ further increases the required forces by another factor of 5–50×. Taken together, the dynamic forces required for extending polymer bilayer membranes are estimated to be ~40–400× greater than for lipid membranes. These effects suggest that dynamic forces in excess of 160 pN would be required to extract polymer nanotubes. In practice, the required pulling forces are lower than predicted, both for lipid[14] and polymer[19] nanotubes. Previous demonstrations of

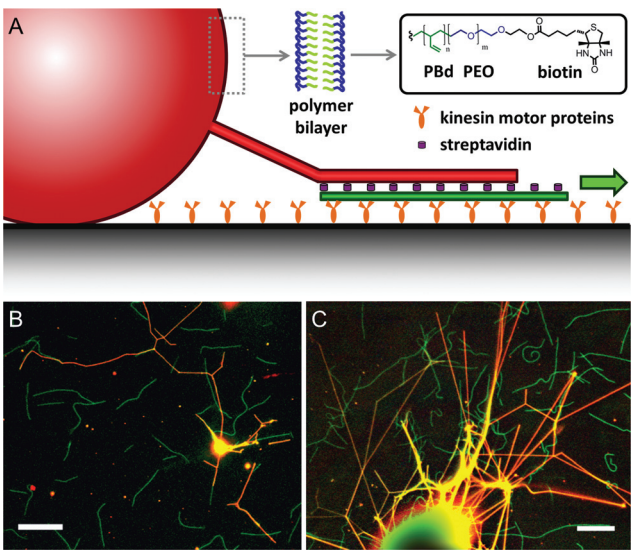

Fig. 1 Schematic representation of the kinesin/microtubule system pulling polymer nanotubes from multilamellar polymersomes (A). Fluorescence photomicrographs of the polymer nanotube networks (red) formed from multilamellar $EO_{21}Bd_{32}$ polymer vesicles and motile microtubules (green), with 8% biotinylated polymer and either 0.5% TRITC-labeled polymer (B) or 0.5% Texas Red-DHPE (C). Scale bars = 10 μm.

‡ The barrier force is comparable to the pulling force when the nanotube diameter is greater than the diameter of the patch of membrane the pulling force acts on.[14] In our experiments, nanotube diameters are on the order of 25–100 nm[13,19] compared to the membrane patch area, presumed to be closer to the microtubule diameter of ~25 nm. In any event, the kinesin/microtubule system is apparently able to overcome this barrier and the relevant force for extending bilayer nanotubes is the dynamic pulling force.

§ Dimova *et al.* reported (see ref. 19) an interfacial coupling constants in the range of 1.1–2.4 × 10^8 dyn s cm^{-3} for polymer bilayers nearly identical to those used in our experiments ($EO_{20}Bd_{32}$ *vs.* $EO_{21}Bd_{32}$), and compared to the range of 4.5–45 × 10^6 dyn s cm^{-3} for DOPC lipids on hexadecyl monolayers as a model for the DOPC bilayer interface.

Published on 24 April 2015. Downloaded by Michigan State University on 20/01/2016 02:28:09.

polymer nanotube extension used optical traps to produce pulling forces on the order of several tens of pictonewtons[13,19] or fluidizing additives[13] to make the polymer more compliant to the mechanical stresses arising from the applied pulling force.

As previously noted with the extraction of lipid nanotubes, the velocity of microtubules attached to polymer nanotubes was strongly dependent on their length. A threshold length of approximately 10 microns was reported at which the velocity of microtubules pulling lipid nanotubes reached the untethered velocity.[5] This dependency on microtubule length reflects the additive force of the kinesin motors acting on a microtubule, which increases proportionally with increasing length. Longer microtubules, thus, are able to exert larger forces during nanotube extraction. In the present study, microtubules with lengths of 15 and 95 μm and extracting polymer nanotubes displayed velocities that were ~45 and 88% that of untethered microtubules. This result suggests that the dynamic forces required to pull and extend polymer nanotubes is significantly greater than that required for lipid nanotubes, where even long microtubules (>90 microns) experience a significant opposing force. This observation is also consistent with the expected increase in force due to the increased membrane thickness and interfacial coupling in polymer bilayers as discussed above.

In addition to the higher force requirements to produce polymer nanotube networks, another consequence of the enhanced stability of polymer vesicle membranes is an apparent tradeoff with lateral fluidity, resulting in generally slower diffusive transport compared to lipid membranes. This tradeoff has been observed in fluorescence recovery (FRAP) experiments measuring the 2D lateral diffusion in vesicle membranes,[21] and can be attributed to the substantially higher effective viscosity of polymer membranes.[19] We observed similar effects in the membranes of nanotubes using FRAP (Fig. 2). Here, the fluorescence recovery profiles in one-

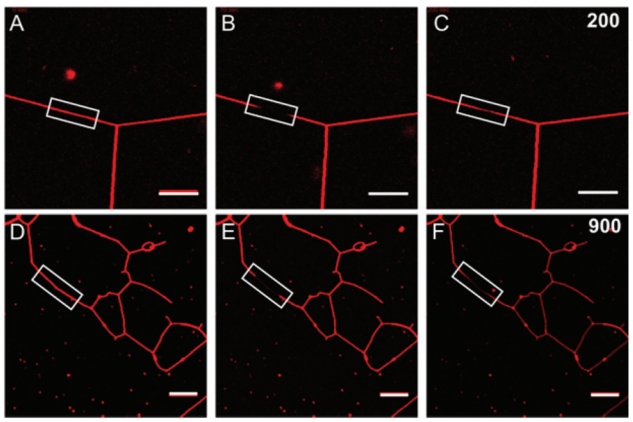

Fig. 2 Fluorescence recovery after photobleaching experiments applied to nanotubes pulled from multilamellar vesicles by motile microtubules (not visible). Fluorescence micrographs of networks composed of lipid (DOPC; A–C) or polymer ($EO_{21}Bd_{32}$; D–F) nanotubes before (A, D), immediately after (B, E), and 200 s (C) or 900 s (F) after photobleaching. Scale bars = 10 μm.

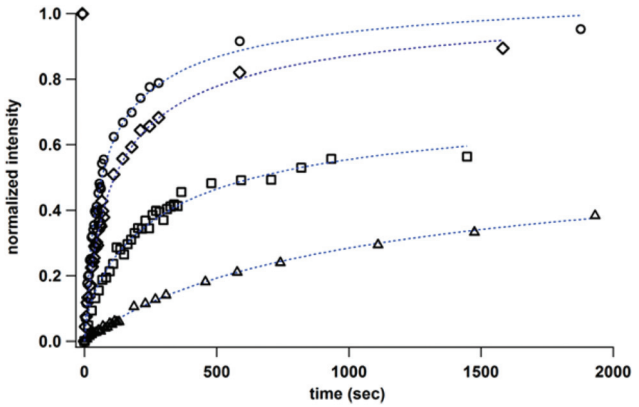

Fig. 3 Fluorescence recovery profiles for 0.5% TR-DHPE in DOPC nanotubes (○); 0.5% tetramethylrhodamine-$EO_{21}Bd_{32}$ in polymer nanotubes (△). Also shown are recovery profiles for 0.5% TR-DHPE in polymer nanotubes with (□) and without (◊) sQDs.

dimensional nanotubes pulled from MLVs (Fig. 3) were fit to a 1D model[22] (see Experimental section) to determine diffusion coefficients of the fluorescent tracers. Not surprisingly, the diffusion coefficient of TRITC-labeled polymer chains in $EO_{21}Bd_{32}$ polymer nanotubes (0.015 $\mu m^2\ s^{-1}$) was considerably slower than the lipid-dye TR-DHPE in DOPC lipid nanotubes (0.29 $\mu m^2\ s^{-1}$), a decrease of ~20-fold. Additionally, the 1D fluorescence recovery was 10× slower in nanotubes pulled from MLVs as compared to the 2D recovery observed[20] in vesicle (either polymer or lipid) membranes. The reduced diffusivity in nanotube membranes has been observed previously for 1D lipid bilayers formed over carbon nanotubes,[23] and may reflect a diameter-dependent lateral diffusion in membrane nanotubes.[24] Nevertheless, both polymer and lipid nanotube membranes exhibit lateral fluidity that is consistent in relative magnitude with fluidity observed in corresponding planar membranes.

While the mobility and fluorescence recovery observed in polymeric systems were not related to the biomolecular crosslinking of the biotin–streptavidin interactions (*i.e.* free streptavidin is removed from solution prior to adding polymer MLVs), we observed that the transport of materials in polymer nanotubes could be modulated by introducing such interactions. Polyvalent streptavidin-coated quantum dots (sQDs), for example, would be expected to link multiple biotinylated membrane components. Previously, we characterized the lateral 1D mobility of streptavidin-coated quantum dots (sQDs) along lipid nanotube networks.[5] In stark contrast, comparable loadings of sQDs added to polymer nanotubes comprised of 8% biotinylated $EO_{21}Bd_{32}$ were able to bind to the nanotube but did not exhibit lateral diffusion. Mean-squared displacement measurements confirmed that the bound sQDs were immobile (Fig. 4A) on observational timescales. These data strongly suggest that biomolecular crosslinking resulted in the accumulation of biotinylated polymer chains by the sQDs into larger structures, and therefore slowing or ceasing diffusion. A closer examination of the MSD data indicated that the reduced mobi-

 This journal is © The Royal Society of Chemistry 2015

Published on 24 April 2015. Downloaded by Michigan State University on 20/01/2016 02:28:09.

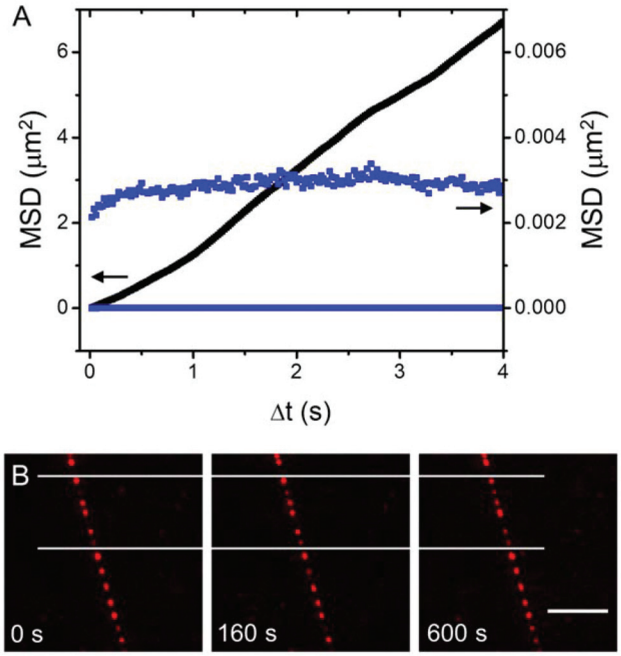

Fig. 4 (A) Plot of the mean-squared displacement for streptavidin-coated quantum dots captured on $EO_{21}Bd_{32}$ nanotubes with 8% biotinylated polymer chains (blue) and compared to previously reported (see ref. 5) MSD of QDs on lipid nanotubes (black). Secondary *y*-axis indicates scale for the sQD/polymer MSD data (blue squares). (B) Fluorescence micrographs of captured sQDs (red) on polymer nanotubes initially, and after 160 and 600 s. Parallel lines added as a guide to the eyes. Scale bar 10 μm.

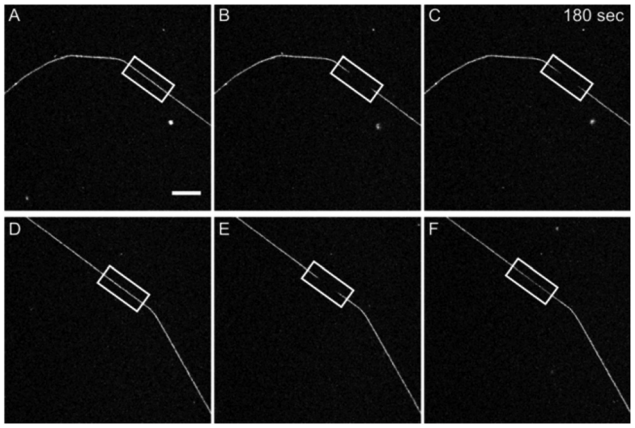

Fig. 5 Fluorescence recovery after photobleaching of a 0.5% TR-DHPE in $EO_{21}Bd_{32}$ nanotube with 8% biotinylated polymer chains with streptavidin-coated quantum-dots (A–C) and without (D–F) before (A, D), immediately after (B, E) and 180 s after (C, F) photobleaching a 10 μm section of the nanotubes. Scale bar 10 μm.

lity is not merely an attenuation due to a reduced diffusion coefficient (linear MSD), or due to restricted single-file diffusion (in which MSD scales with $t^{1/2}$);[25,26] rather, there is a complete inhibition of lateral diffusion. Indeed, fluorescence microscopy confirmed that sQDs were completely immobile over timescales of at least 10 min (Fig. 4B). This complete interruption of lateral diffusion by sQDs along polymer nanotubes was surprising and contrasts sharply with the modest (but expected) 20-fold decrease in diffusion in lipid nanotube membranes with a comparable fraction of biotinylated lipids. A similar lack of diffusion has been observed in polymer bilayers supported on glass surfaces,[27,28] which suggests a significant coupling between polymer chains comprising the membrane that could be exacerbated by the *in situ* formation of significantly larger polymer aggregates following the introduction of sQDs.

A critical question is to what extent the *in situ* creation of such immobile structures (*i.e.* sQDs linked to multiple biotinylated polymer chains) affects the transport of other non-biotinylated membrane components in the polymer nanotube. While the sQDs themselves remain immobile, FRAP experiments revealed that the much smaller fluorescently-labeled lipids that do not supramolecularly interact with sQDs are still able to laterally diffuse in this system (Fig. 5). The rate of diffusion of these lipids, however, is considerably slower as a consequence of the obstruction of the larger and immobile obstacles.[29] Indeed the diffusion coefficients estimated from fits to the fluorescence recovery data (Fig. 3) with (0.17 μm^2 s^{-1}) and without captured sQDs (0.30 μm^2 s^{-1}) reflects a relative decrease to approximately one-half. This decrease is much greater than expected[29] for an immobile fraction of 8% (*i.e.* the experimental upper limit based on the fraction of biotinylated polymer chains). The magnitude of the reduction in lateral diffusion suggests an enhanced sensitivity of diffusive transport to immobile obstacles in membranes that should be considered when designing membrane nanotube transport systems.

Conclusions

The motivations for this work included expanding the library of materials that can be used to rapidly prepare large-scale nanotube networks, and enhancing our understanding of materials transport along the nanotube highways. Indeed, we have shown that despite higher forces required to deform polymer membranes, the forces generated by kinesin/microtubule transport are able to pull nanotubes and generate large-scale networks, without the need for a fluidizing material. Certainly other vesicle-forming polymers and molecules may also be used to generate networks, according to their relevant physical parameters (*e.g.* membrane thickness, bending rigidity and interfacial coupling). Nevertheless, the increased effective membrane viscosity in PEO-PBd nanotube networks is manifested in the slower transport properties of components diffusing in the polymer membranes. FRAP analysis also revealed differences in the diffusivity based on the dimensionality (*i.e.*, 1D *vs.* 2D) of the lipid and polymer structures. Although reduced transport in polymer membranes is not entirely unexpected,[21] we observed that this effect is greatly

Published on 24 April 2015. Downloaded by Michigan State University on 20/01/2016 02:28:09.

exacerbated in the presence of polyvalent QDs, capable of linking many complementary-functionalized polymer chains into larger and less mobile membrane-bound structures. The formation of such larger structures results in virtually immobile nanotube-adsorbed QDs. These membrane-aggregated structures act effectively as less-mobile obstacles that substantially reduce the membrane-based transport of materials along the polymer nanotubes. Such effects should be taken into account when designing membrane-based transport systems in synthetic systems that mimic biological transport highways. Nevertheless, it is important to note that the polymer nanotube membranes are capable of transporting small molecules along nanotube conduits and the marginal decrease in intramembrane transport rates may be offset by the enhanced stability of polymer nanotube networks.

Experimental

Inverted motility assay

Microtubules polymerized with 5% biotinylated tubulin were added to a capillary flow chamber containing kinesin-coated surfaces kept at 23 °C. Commonly, this setup is referred to as the inverted motility assay (IMA) for kinesin and actin molecular motors. A 1.7 μM streptavidin solution was then added into the flow cell to create fully coated streptavidin microtubules.[30] After excess streptavidin was removed, microtubules were observed to undergo normal motile behavior and translocated on the surface of the chamber with an average velocity of 0.42 ± 0.01 μm s^{-1}. Here, the concentration of kinesin motors (325 nM) and length of the microtubules (>2 μm) satisfy the criteria for near perpetual microtubule surface motion.[31] There is no initial preferential orientation of the surface-adsorbed microtubule, and their trajectories follow random walk statistics at sufficient time scales.[32] Polymer MLVs – containing 8% biotin-$EO_{21}Bd_{32}$ and 0.5% of either tetramethylrhodamine-$EO_{21}Bd_{32}$ or Texas Red DHPE – were then added to the flow cell. The IMA with polymer MLVs was then incubated inside the flow cell and imaged by fluorescence microscopy.

Synthesis of biotin-$EO_{21}Bd_{32}$

Biotin (244 mg) was dissolved in 12 mL of dry dimethylformamide and added to a 50 mL round bottom flask equipped with as stirbar and septum. Next, 2 mL of 1 M *N*,*N*′-dicyclohexylcarbodiimide in methylene chloride was added to through the septum of the flask and the mixture was sparged with dry nitrogen for 15 minutes. Then, poly(ethylene oxide)$_{21}$-*b*-poly(butadiene)$_{32}$ (260 mg) was dissolved in 6 mL of chloroform and added to the flask through the septum. The resulting mixture was stirred at room temperature for 3 h under nitrogen. At the end of this time, the solvent was removed *in vaccuo* and replaced with 5 mL tetrahydrofuran. The polymer was purified by preparatory GPC and the solvent removed, yielding 220 mg (93%) of the purified biotinylated polymer. NMR (500 MHz, $CDCl_3$): δ = 5.75–5.2 (64H, broad, poly(butadiene) CH═CH_2), 4.95 (32H, broad, poly(butadiene) C*H*═CH_2), 4.54 (1H, m, biotin –C*H*(CH_2–)NHC(O)–), 4.38 (1H, m, –C*H*(CH-(CH_2–)–)NHC(O)–), 4.16 (2H, m, PEO–CH_2–C(O)–biotin) 3.8–3.5 (82H, PEO backbone), 2.93 (1H, –SC*H*H′–CH(–CH)–NHC(O)–), 2.76 (1H, –SC*H*H′–CH(–CH)–NHC(O)–), 2.25–1.5 (64H, broad m, butadiene backbone), 1.5–1 (32H, broad m, butadiene backbone), 0.84 (8H, m, initiator fragment). The end functionality was determined to be 78% by NMR.

Synthesis of tetramethylrhodamine-$EO_{21}Bd_{32}$

To prepare tetramethylrhodamine-$EO_{21}Bd_{32}$, we modified an existing procedure.[21] To a 25 mL round bottom flask were added 100 mg of the copolymer and the molar equivalent of TRITC, along with 10 mL of toluene. The mixture was sparged with N_2 and refluxed under nitrogen overnight. The toluene was then removed *in vaccuo* and the resulting solid was purified *via* prep-column chromatography. A UV-Vis survey of the extinction coefficient (λ = 551 nm) in methanol was compared to existing data for free TRITC (100 000 M^{-1} cm^{-1} @544 nm in methanol) and was used to estimate that the polymer was 5% functionalized with dye.

Formation of polymer multilamellar vesicles

Biotin-$EO_{21}Bd_{32}$ (1 mg) was mixed with unfunctionalized $EO_{21}Bd_{32}$ (9 mg) and dissolved in 1 mL of chloroform. To this solution 100 μL of 1 mM Texas Red DHPE in chloroform was added. This solution was carefully pipetted down the inside of a 25 mL round bottomed flask containing 10 mL of aqueous BRB80 buffer so that an unperturbed two-phase system resulted. The chloroform layer was slowly evaporated at 40 °C using a rotary evaporator. Reduced pressure (~470 mbar) was used initially and until the majority of chloroform was removed. The vacuum was then increased (~80 mbar) to remove remaining chloroform. The resulting vesicle suspension was stored in a 4 °C refrigerator in the dark and used within 2 weeks. Vesicles containing dye-functionalized polymer were created using the same techniques, except that 1 mg of the 5% tetramethylrhodamine-$EO_{21}Bd_{32}$ was added to 8 mg unfunctionalized polymer and 1 mg of biotinylated polymer. No Texas Red DHPE was added to this sample.

Fitting fluorescence recovery profiles

We fit the normalized fluorescence intensity profiles to the equation given by Shaklee *et al.* for 1D diffusion of a membrane dye,[22] and included a term to account for the possibility of an immobile fraction:[33]

$$F(t) = I_{\text{final}} w \left(1 - \frac{4t^{1/2}\left(\exp\left(\frac{-\tau_D}{16t}\right) - 1\right)}{(\tau_D \pi)^{1/2}} - \text{Erf}\left(\frac{1}{4}\left(\frac{\tau_D}{t}\right)^{1/2}\right)\right) \times \left(\frac{I_{\text{final}} - I_{\text{bleach}}}{I_{\text{initial}} - I_{\text{bleach}}}\right)$$

where I_{final} is the asymptotic value of maximum fluorescence recovery, w is the width of the bleached region, t is the time, $\tau_D = w^2/D$ and D is the diffusion coefficient of the fluorophore in

 This journal is © The Royal Society of Chemistry 2015

Published on 24 April 2015. Downloaded by Michigan State University on 20/01/2016 02:28:09.

the membrane, and $I_{initial}$ and I_{bleach} are the measured intensities of the probe region before and after photobleaching. The final term $(I_{final} - I_{bleach})/(I_{initial} - I_{bleach})$ is the mobile fraction. We fit the data with two adjustable parameters: the diffusion coefficient, and the mobile fraction. Fits to this model converged with mobile fractions of 1 for both the lipid dye in lipid nanotubes and the lipid dye in polymer nanotubes without QDs, and to 0.7 for both the lipid in polymer with QDs and the polymer dye in polymers.

Nanoparticle capture and diffusivity

To the stopped networks, 1 : 100 diluted concentrations of Qdot 605 streptavidin coated nanocrystals in AMP-PNP motility solution. Qdot diffusivity was observed at 60 fps. Image processing and particle tracking were performed in Fiji released under the General Public License.[34,35]

Acknowledgements

This work was supported by the U.S. Department of Energy, Office of Basic Energy Sciences, Materials Sciences and Engineering Division (BES-MSE). N.F. Bouxsein (polymer network assembly, characterization, and data analysis), W.F. Paxton (polymersome preparation and data analysis), A. Gomez (polymersome preparation and network assembly) and G.D. Bachand (kinesin/microtubule motility and analysis) were supported BES-MSE. I.M. Henderson (polymer synthesis and functionalization) was supported through the Center for Integrated Nanotechnologies. This work was performed, in part, at the Center for Integrated Nanotechnologies, an Office of Science User Facility operated for the U.S. Department of Energy (DOE) Office of Science (user project number U2012A0072). Sandia National Laboratories is a multi-program laboratory managed and operated by Sandia Corporation, a wholly owned subsidiary of Lockheed Martin Corporation, for the U.S. Department of Energy's National Nuclear Security Administration under contract DE-AC04-94AL85000.

Notes and references

1 B. Alberts, A. Johnson, J. Lewis, M. Raff, K. Roberts and P. Walter, *Molecular Biology of the Cell*, Garland Science, New York, 5th edn, 2008.
2 C. Leduc, O. Campas, K. B. Zeldovich, A. Roux, P. Jolimaitre, L. Bourel-Bonnet, B. Goud, J. F. Joanny, P. Bassereau and J. Prost, *Proc. Natl. Acad. Sci. U. S. A.*, 2004, **101**, 17096.
3 A. Roux, G. Cappello, J. Cartaud, J. Prost, B. Goud and P. Bassereau, *Proc. Natl. Acad. Sci. U. S. A.*, 2002, **99**, 5394.
4 C. Leduc, O. Campas, J. F. Joanny, J. Prost and P. Bassereau, *Biochim. Biophys. Acta, Biomembr.*, 2010, **1798**, 1418.
5 N. F. Bouxsein, A. Carroll-Portillo, M. Bachand, D. Y. Sasaki and G. D. Bachand, *Langmuir*, 2013, **29**, 2992.
6 M. Karlsson, K. Sott, M. Davidson, A. S. Cans, P. Linderholm, D. Chiu and O. Orwar, *Proc. Natl. Acad. Sci. U. S. A.*, 2002, **99**, 11573.
7 J. E. Reiner, R. Kishore, C. Pfefferkorn, J. Wells, K. Helmerson, P. Howell, W. Vreeland, S. Forry, L. Locasio, D. Reyes-Hernandez and M. Gaitan, in *Optical Trapping and Optical Micromanipulation*, ed. K. Dholakia and G. C. Spalding, SPIE-The International Society for Optical Engineering, Bellingham, 2004, vol. 5514, p. 246.
8 S. Pande, S. Shitut, L. Freund, M. Westermann, F. Bertels, C. Colesie, I. B. Bischofs and C. Kost, *Nat. Commun.*, 2015, 6.
9 G. P. Dubey and S. Ben-Yehuda, *Cell*, 2011, **144**, 590.
10 B. M. Discher, Y. Y. Won, D. S. Ege, J. C. M. Lee, F. S. Bates, D. Discher and D. A. Hammer, *Science*, 1999, **284**, 1143.
11 D. E. Discher and F. Ahmed, *Annu. Rev. Biomed. Eng.*, 2006, **8**, 323.
12 D. E. Discher and A. Eisenberg, *Science*, 2002, **297**, 967.
13 J. Reiner, J. M. Wells, R. B. Kishore, C. Pfefferkorn and K. Helmerson, *Proc. Natl. Acad. Sci. U. S. A.*, 2006, **103**, 1173.
14 G. Koster, A. Cacciuto, I. Derenyi, D. Frenkel and M. Dogterom, *Phys. Rev. Lett.*, 2005, **94**, 068101.
15 E. Evans and A. Yeung, *Chem. Phys. Lipids*, 1994, **73**, 39.
16 G. Srinivas, D. E. Discher and M. L. Klein, *Nat. Mater.*, 2004, **3**, 638.
17 H. Bermudez, A. K. Brannan, D. A. Hammer, F. S. Bates and D. E. Discher, *Macromolecules*, 2002, **35**, 8203.
18 H. I. Petrache, S. Tristram-Nagle, K. Gawrisch, D. Harries, V. A. Parsegian and J. F. Nagle, *Biophys. J.*, 2004, **86**, 1574.
19 R. Dimova, U. Seifert, B. Pouligny, S. Forster and H. G. Dobereiner, *Eur. Phys. J. E: Soft Matter Biol. Phys.*, 2002, **7**, 241.
20 R. Merkel, E. Sackmann and E. Evans, *J. Phys.*, 1989, **50**, 1535.
21 J. C. M. Lee, M. Santore, F. S. Bates and D. E. Discher, *Macromolecules*, 2002, **35**, 323.
22 P. M. Shaklee, L. Bourel-Bonnet, M. Dogterom and T. Schmidt, *Biophys. J.*, 2010, **98**, 93.
23 A. B. Artyukhin, A. Shestakov, J. Harper, O. Bakajin, P. Stroeve and A. Noy, *J. Am. Chem. Soc.*, 2005, **127**, 7538.
24 D. R. Daniels and M. S. Turner, *Langmuir*, 2007, **23**, 6667.
25 T. E. Harris, *J. Appl. Probab.*, 1965, **2**, 323.
26 L. Lizana and T. Ambjornsson, *Phys. Rev. E: Stat., Nonlinear, Soft Matter Phys.*, 2009, **80**, 051103.
27 M. Goertz, L. E. Marks and G. A. Montano, *ACS Nano*, 2012, **6**, 1532.
28 D. L. Gettel, J. Sanborn, M. A. Patel, H.-P. de Hoog, B. Liedberg, M. Nallani and A. N. Parikh, *J. Am. Chem. Soc.*, 2014, **136**, 10186.
29 M. J. Saxton, *Biophys. J.*, 1987, **52**, 989.
30 S. He, A. T. Lam, Y. Jeune-Smith and H. Hess, *Langmuir*, 2012, **28**, 10635.
31 J. Howard, A. J. Hudspeth and R. D. Vale, *Nature*, 1989, **342**, 154.

32 T. Duke, T. E. Holy and S. Leibler, *Phys. Rev. Lett.*, 1995, **74**, 330.
33 D. Axelrod, D. E. Koppel, J. Schlessinger, E. Elson and W. W. Webb, *Biophys. J.*, 1976, **16**, 1055.
34 M. H. Longair, D. A. Baker and J. D. Armstrong, *Bioinformatics*, 2011, **27**, 2453.
35 J. Schindelin, I. Arganda-Carreras, E. Frise, V. Kaynig, M. Longair, T. Pietzsch, S. Preibisch, C. Rueden, S. Saalfeld, B. Schmid, J. Y. Tinevez, D. J. White, V. Hartenstein, K. Eliceiri, P. Tomancak and A. Cardona, *Nat. Methods*, 2012, **9**, 676.

Published on 24 April 2015. Downloaded by Michigan State University on 20/01/2016 02:28:09.

This journal is © The Royal Society of Chemistry 2015